Received: December 20, 2016

International Journal of
Intelligent Engineering & Systems

http://www.inass.org/

Fuzzy Sliding Mode Controller of DFIG for Wind Energy Conversion

Ouassila Belounis [1]* **Hocine Labar [2]**

[1] *Department of Electrical Engineering, University Badji Mokhtar Annaba, PB 12, 23000 Annaba, Algeria*
[2] *Laboratoire d'Electrotechnique d'Annaba (LEA), Department of Electrical Engineering, University Badji Mokhtar Annaba, PB 12, 23000 Annaba, Algeria*
* Corresponding author's Email: belounisouassila@yahoo.fr

Abstract: Wind turbine based on Doubly-Fed Induction Generator (DFIG) is gaining in the growing wind market. This paper describes a design method for the fight control of doubly-fed induction generator (DFIG) based on fuzzy sliding mode control, based on the coupling of the fuzzy logic control and sliding mode control. This technique is defined on general, yet detailed. To ensure this requirement a detailed decoupled modeling of DFIG is presented. The relationship between the control parameters and the desired active and reactive power is provided and tested. The main goal achieved by the control strategy is to control the amount of active and reactive power produced by the doubly fed induction generator and injected in the main grid according to the power references derived from turbine's mechanical power and the grid operator. The results of simulation are conducted to validate the theory and indicate that the control performance of the DFIG is satisfactory and the proposed fuzzy sliding mode control (FSMC) can achieve favorable tracking performance.

Keywords: Doubly-fed induction generator (DFIG), Fuzzy sliding mode vontrol (FSMC), MPPT control, Sliding mode control (SMC), Wind turbine.

1. Introduction

The increasing energy demand, together with the harmful effect of fossil fuel exploitation on the climate and environment, are among the main factors that have boosted worldwide interest in renewable energies. Among a variety of renewable-energy resources, wind power is drawing the most attention from all over world [1]. Doubly Fed Induction Generator (DFIG) is an electrical three phase asynchronous machine with wound rotor accessible for control. As the power handled by the rotor is proportional to the slip, the power electronic converter used in the rotor circuit can be designed for only a fraction of the overall system power. This topology is very attractive for both wind energy generation and high power drive applications [2]. Theoretical analysis, modeling and simulation study are provided.

A Sliding Mode Controller has been applied in many fields due to its excellent properties, such as insensitivity to some external disturbances and parameters variation, sliding mode controller (SMC) can exhibit fast dynamic responses [2]. However, the SMC has a major inconvenience which is the chattering effect created by the discontinuous part of control. In order to resolve this problem, one way to improve sliding mode controller performance is to combine it with Fuzzy Logic (FL) to form a fuzzy sliding mode controller (FSMC) which can be applied to reduce the chattering phenomenon of the SMC controller.

The remainder of this paper is organized as follows: The description of studies system presented in section 2. The dynamic model of the DFIG, wind turbine and gearbox are designed in section 3 and 4 respectively, control strategies were developed to control the active and reactive power in order to maximize the wind energy production. In section 5 the simulation result of this machine is presented.

Received: December 20, 2016

The sliding mode control (SMC) is described in section 6. In section 7 we introduce the FSMC controller (combination between sliding mode and fuzzy logic controls) to the DFIG control and discuss its benefits. The effectiveness of the proposed method verified by simulation is presented in section 8. To demonstrate, the performances of the control strategies are investigated and compared. Finally in the conclusion are set out the essential findings of this work.

2. Description of studied system

The configuration of DFIG connected directly on the grid is shown in figure 1. The stator is directly connected to the Alternative Current (AC) mains, whilst the wound rotor is fed from the power electronics converter via slip rings to allow DFIG to operate at a variety of speeds in response to changing wind speed. Indeed, the basic concept is to interpose a frequency converter between the variable frequency asynchronous generator and fixed frequency grid. The direct current power available at the rectifier Pulse Width Modulation (PWM) output is filtered and converted to AC power using a PWM inverter.

The main advantage of the DFIG is the reduced converter size which depends on the machine's slip and usually does not exceed 25-30% of the machine's nominal power [3]. We use two controllers: Sliding Mode and Fuzzy Sliding Mode in order to show that controllers can improve performances of doubly-fed induction generators.

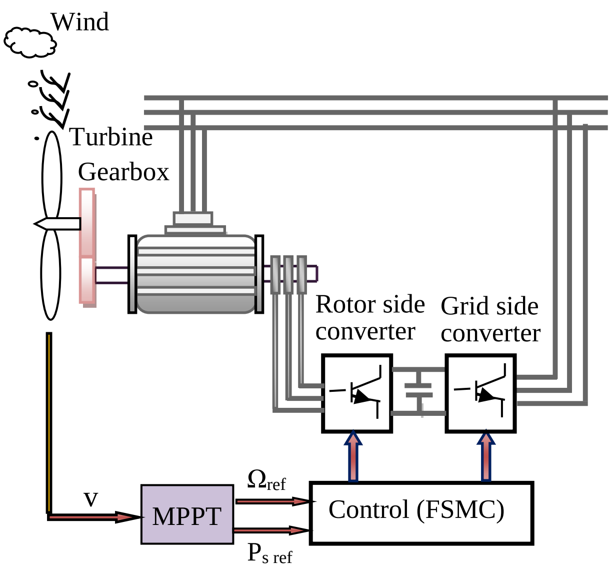

Figure.1 Configuration of DFIG connected directly on the grid.

3. Modeling and control of the DFIG

A classical modeling of the DFIG in the Park reference frame is used. The voltage and flux equations of the DFIG are given as follows[4][6][7]:

$$\begin{cases} V_{sd} = R_s I_{sd} + \dfrac{d}{dt}(\varphi_{sd}) - \omega_s \varphi_{sq} \\ V_{sq} = R_s I_{sq} + \dfrac{d}{dt}(\varphi_{sq}) + \omega_s \varphi_{sd} \\ V_{rd} = R_r I_{rd} + \dfrac{d}{dt}(\varphi_{rd}) - \omega_r \varphi_{rq} \\ V_{rq} = R_r I_{rq} + \dfrac{d}{dt}(\varphi_{rq}) + \omega_r \varphi_{rd} \end{cases} \quad (1)$$

The stator and rotor flux are given as:

$$\begin{cases} \varphi_{sd} = L_s I_{sd} + M\ I_{rd} \\ \varphi_{sq} = L_s\ I_{sq} + M\ I_{rq} \\ \varphi_{rd} = L_r\ I_{rd} + M\ I_{sd} \\ \varphi_{rq} = L_r I_{rq} + M\ I_{sq} \end{cases} \quad (2)$$

Subscripts d and q refer to the d- and q-axes, respectively and subscripts s and r to the stator and rotor of the DFIG respectively; ω_s and ω_r (rad/s) are the stator and rotor variable pulsations respectively; V_{sd}, V_{sq}, V_{rd} and V_{rq} are respectively the direct and quadrature stator and rotor voltages, I_{sd}, I_{sq}, I_{rd} and I_{rq} are the direct and quadrature stator and rotor currents, φ_{sd}, φ_{sq}, φ_{rd} and φ_{rq} are respectively the direct and quadrature components of stator and rotor fluxes; R_s and R_r are stator and rotor resistances; L_s and L_r are the stator and the rotor leakage inductance and M is the magnetizing inductance; p: number of pair poles. The electromagnetic C_{em} torque is expressed as:

$$C_{em} = p(M/L_s)(I_{rd}\varphi_{sq} - I_{rq}\varphi_{sd}) \quad (3)$$

The active and reactive powers at the stator side are defined as [4] [5] [6]:

$$\begin{cases} P_s = V_{sd} I_{sd} + V_{sq} I_{sq} \\ Q_s = V_{sq} I_{sd} - V_{sd} I_{sq} \end{cases} \quad (4)$$

Choosing a biphasic reference frame d-q with the stator vector flux φ_{sd} aligned with the axis d allows getting constant electrical voltages and currents in permanent mode (figure 2).

So, we can write: $\varphi_{sd} = \varphi_s$, $\varphi_{sq} = 0$.

Received: December 20, 2016

The equation of the electromagnetic torque becomes then:

$$C_{em} = -p\,(M/L_s) I_{rq} \varphi_s \quad (5)$$

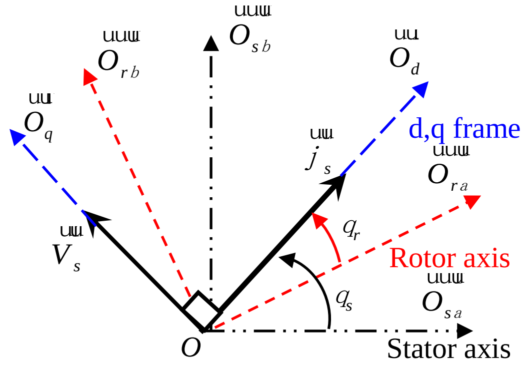

Figure.2 Orientation of the d, q frame [4] [5] [6] [7] [8].

Assuming that the electrical power network to which is connected the DFIG is stable, the flux φ_{sd} becomes constant.

The choice of this reference frame makes the electromagnetic torque produced by the machine and consequently the active power dependent only on the rotor current of axis *q*.

$$\begin{cases} V_{sd} = 0 \\ V_{sq} = V_s = \omega_s \varphi_s \end{cases} \quad (6)$$

In this case, the equations of flux can be expressed as follow:

$$\begin{cases} \varphi_s = L_s I_{sd} + M\, I_{rd} \\ 0 = L_s I_{sq} + M\, I_{rq} \end{cases} \quad (7)$$

$$\begin{cases} I_{sd} = \dfrac{-M}{L_s} I_{rd} + \dfrac{\varphi_s}{L_s} \\ I_{sq} = \dfrac{-M}{L_s} I_{rq} \end{cases} \quad (8)$$

From equations (4) and (6) the stator active and reactive powers become:

$$\begin{cases} P_s = V_{sq} I_{sq} \\ Q_s = V_{sq} I_{sd} \end{cases} \quad (9)$$

By replacing I_{sd} and I_{sq} by their expressions given in equation (8),

$$\Rightarrow \begin{cases} P_s = -V_s (M/L_s) I_{rq} \\ Q_s = -V_s (M/L_s) I_{rd} + (V_s \varphi_s / L_s) \end{cases} \quad (10)$$

The equations of rotor flux can be expressed as follow:

$$\begin{cases} \varphi_{rd} = I_{rd}\left(L_r - \dfrac{M^2}{L_s}\right) + \left(\dfrac{V_s M}{\omega_s L_s}\right) \\ \varphi_{rq} = I_{rq}\left(L_r - \dfrac{M^2}{L_s}\right) \end{cases} \quad (11)$$

In steady state mode, the terms containing the derivative of biphasic rotor currents disappear, so:

$$\begin{cases} V_{rd} = R_r I_{rd} - g\,\omega_s\left(I_{rq}\left(L_r - \dfrac{M^2}{L_s}\right)\right) \\ V_{rq} = R_r I_{rq} + g\,\omega_s\left(I_{rd}\left(L_r - \dfrac{M^2}{L_s}\right)\right) + g\,\dfrac{V_s M}{L_s} \end{cases} \quad (12)$$

4. Modeling of the wind turbine and gearbox

The mechanical power available on the turbine shaft, extracted from the wind is given by [8] [9]:

$$P_m = \frac{1}{2} C_P\, \rho\, \pi\, R^2 v^3 \quad (13)$$

The speed ratio λ is defined like follow [4] [9]:

$$\lambda = \Omega_t \frac{R}{v} = \Omega_{mec} \frac{R}{G\,v} \quad (14)$$

Where, R is the radius of the turbine (m), ρ is the air density (kg/m^3), v is the wind speed (m/s). In this work, the C_P equation is approximated using a non-linear function according to [10].

$$C_p(\lambda,\beta) = (0.5 - 0.0167(\beta-2))\sin\left[\frac{\pi\,(\lambda+0.1)}{18.5 - 0.3\,(\beta-2)}\right] - 0.00184\,(\lambda-3)(\beta-2) \quad (15)$$

C_P is the power coefficient which is a function of both tip speed ratio λ, and blade pitch angle β (deg). A schema showing the relation between C_P, β and λ is presented in figure 3. The maximum value of C_p ($C_{P\,max} = 0.5$) is achieved for $\beta = 2$ degree and for $\lambda_{opt} = 9.2$.

Received: December 20, 2016

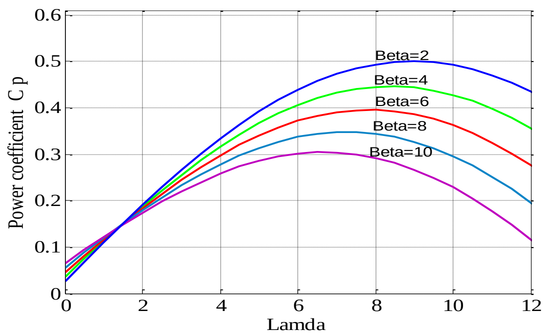

Figure.3 Non linear curve in terms of λ in place of different β.

A wind turbine C_t is characterized by its aero dynamical torque, which is given by [6]:

$$C_t = \frac{P_m}{\Omega_t} = \frac{(0.5 C_p \rho \pi R^2) v^3}{\Omega_t} \tag{16}$$

The wind turbine model can be represented as figure 4:

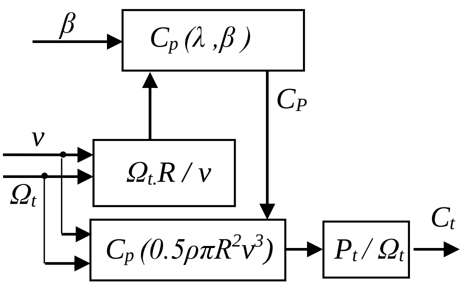

Figure.4 Model of the wind turbine.

4.1 MPPT control strategy

For operating at variable speed in order to recover the maximum of power of the turbine (figure 1) several techniques can be used: for our indirect control [11]:

$$C_{t-opt} = \frac{1}{2} \rho \pi R^3 v^2 \frac{C_P(\lambda_{opt})}{\lambda_{opt}} \tag{17}$$

$$C_{g-opt} = \frac{1}{2G} \rho \pi R^3 v^2 \frac{C_P(\lambda_{opt})}{\lambda_{opt}} \tag{18}$$

This control is based on an estimate of the wind speed. Where the wind torque C_t is given as [11]:

$$C_{t-opt} = \frac{1}{2} \rho \pi R^5 \frac{C_P(\lambda_{opt})}{\lambda_{opt}^3} \Omega_t^2 = K_{opt} \Omega_t^2 \tag{19}$$

C_{t-opt}: The optimal torque of wind turbine, λ_{opt}: Optimal speed ratio, C_{g-opt}: The optimal torque of generator.

In steady state, the mechanical equation can be written in the form:

$$\frac{C_t}{G} - C_g - f\,\Omega_g = 0 \tag{20}$$

Replacing C_t by its expression:

$$C_{g-opt} = \frac{K_{opt}}{G^3} \Omega_g^2 - f\,\Omega_g \tag{21}$$

With: $\Omega_g = G\,\Omega_t$

Below the rated power, the system runs in maximum power tracking mode (figure 5).

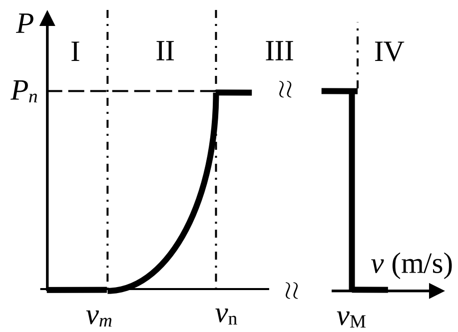

Figure.5 Operating regions of generated power.

The block diagram of the control structure is presented in the figure 6.

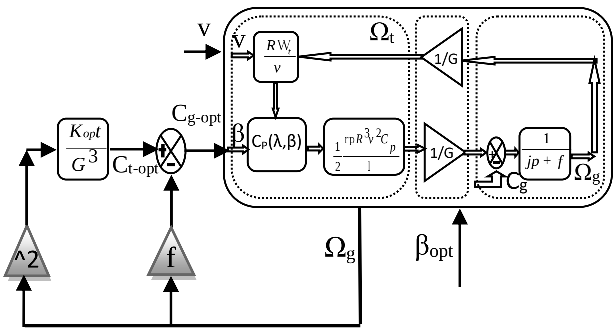

Figure.6 Indirect control speed (Zone II).

It consists to track the rotor speed with changing wind velocity so that the power coefficient (C_{Pmax}) is always maintained at its maximum value [6].

 DOI: 10.22266/ijies2017.0430.18

Received: December 20, 2016

5. Simulation

All simulations were done using MATLAB software for 10 seconds and in all of them, wind speed profile (based on the model presented in figure 1) has been shown in figure 7. This figure illustrates the simulation waveforms of the wind turbine. The figure 7.(a) represents the available wind speed, the power coefficient C_P of the wind turbine and its reference are represented in figure 7.(b), figure 7.(c) : Rotor speed (mechanical).

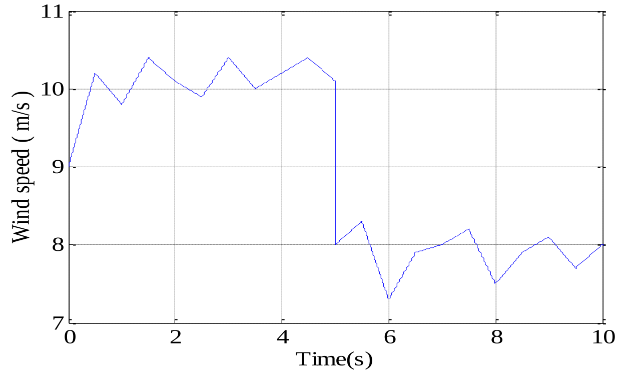

(a)

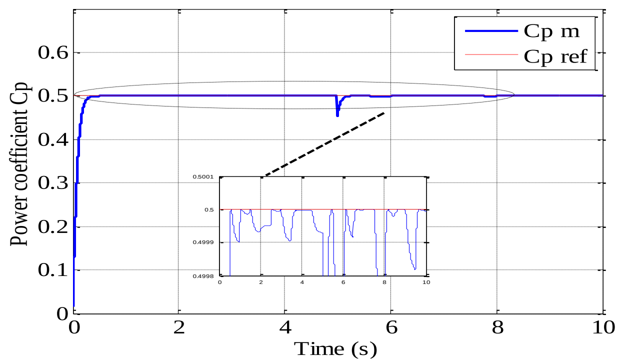

(b)

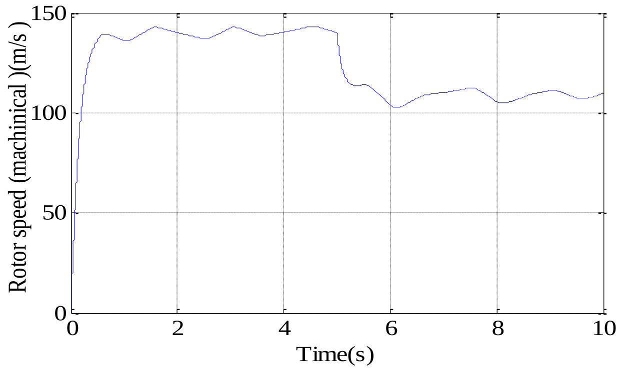

(c)

Figure.7 Simulation waveforms of the wind turbine, (a): Wind speed (m/s), (b): C_p of the wind turbine and its reference, (c): Rotor speed (mechanical).

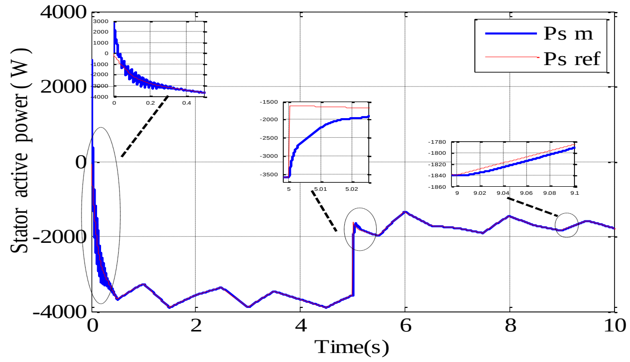

(a)

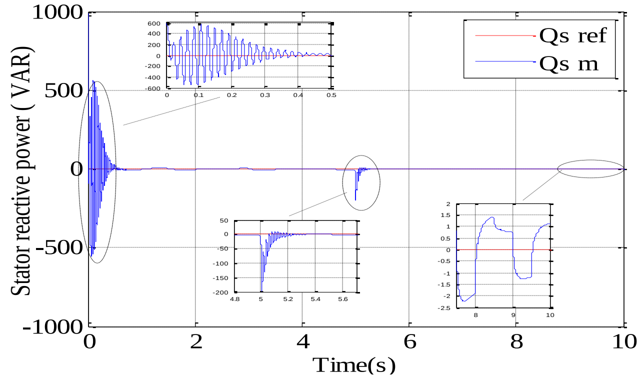

(b)

Figure.8 Reference and measured power of the DFIG, (a): active power, (b):reactive power.

The stator active power set-point is inspired from the MPPT bloc. The stator active and reactive power and its reference are shown in figure 8. The stator reactive power is controlled to be zero during all modes.

6. Sliding Mode Control (SMC)

The main arguments in favor of sliding mode control are order reduction, decoupling design procedure, disturbance rejection, insensitivity to parameter variations, and simple implementation by means of power converters [12] [13]. Considering the system to be controlled described by state-space equation [14]:

$$\dot{x}(t) = f(x,t) + g(x,t)u \tag{22}$$

The desired control vectors force the trajectory of the system to converge towards the surface defined by [3]:

$$S_{PQ}(x) = 0 \tag{23}$$

The implementation of this control method requires three main steps [13] [14]:

Step1: Choice of control surface

Slotine proposes [15] a surface of sliding which is a scalar function such that the controlled variable slips on the surface:

$$S\left(x\right)=\left(\frac{d}{dt}+\xi\right)^{r-1}e\left(x\right) \tag{24}$$

Where r is the relative degree of the system, ξ is a positive constant and $e\ (x)$ is the error between the variable and its reference. For the considered application, two sliding surfaces are defined as:

$$S\left(P\right)=\left(I_{rq}^{ref}-I_{rq}\right) \tag{25}$$

$$S\left(Q\right)=\left(I_{rd}^{ref}-I_{rd}\right) \tag{26}$$

Step 2: Conditions for convergence

In order to force the chosen variables to converge to their reference values it needs that both surfaces of sliding are driven to zero.

$$\begin{cases} S\left(P\right)=0 \\ S\left(Q\right)=0 \end{cases} \Rightarrow \begin{cases} \dot{S}(P)=\dfrac{d}{dt}\left(I_{rq}^{ref}-I_{rq}\right)=0 \\ \dot{S}(Q)=\dfrac{d}{dt}\left(I_{rd}^{ref}-I_{rd}\right)=0 \end{cases} \tag{27}$$

Step 3: Control law design

The structure of a sliding mode controller consists of two parts. One concerning the exact linearization (u^{eq}) and the other one concerns the stability (u^{n}) [13]. The latter is used to eliminate the effects of imprecision of the model and to reject external disturbances.

$$\begin{cases} u_{rq}=u_{rq}^{eq}+u_{rq}^{n} \\ u_{rd}=u_{rd}^{eq}+u_{rd}^{n} \end{cases} \tag{28}$$

$$\begin{cases} u_{rq}^{n}=-\mathrm{k}_1.sat\left(S\left(P\right)\right) \\ u_{rd}^{n}=-\mathrm{k}_2.sat\left(S\left(Q\right)\right) \end{cases} \tag{29}$$

$$sat\left(S\left(x\right)/\phi\right)=\begin{cases} sign(S) & if\ \left|S\right|>\phi \\ S/\phi & if\ \left|S\right|<\phi \end{cases} \tag{30}$$

Where

u_{rd}, u_{rq}: The control variables,

u_{rd}^{eq}, u_{rq}^{eq} : The equivalent control variables,

u_{rd}^{n}, u_{rq}^{n} : The discontinues control variables,

$sat\ (S(x)/\phi)$: Saturation function,

ϕ: Width of the threshold of the function saturation.

The relation between stator powers and current rotor is given by:

$$\begin{cases} I_{rq}^{ref}=-\dfrac{L_s}{V_s.M}P_s^{ref} \\ I_{rd}^{ref}=\dfrac{V_s}{\omega_s.M}-\dfrac{L_s}{V_s.M}Q_s^{ref} \end{cases} \tag{31}$$

According to (1) and (2), $\dot{I}_{rd}$ and $\dot{I}_{rq}$ can be expressed as:

$$\begin{cases} \dot{I}_{rd}=\left(V_{rd}-R_rI_{rd}+g\,\omega_sL_r\,\sigma\,I_{rq}\right)\dfrac{1}{L_r\sigma} \\ \dot{I}_{rq}=\left(V_{rq}-R_rI_{rq}-g\,\omega_sL_r\sigma I_{rd}-g\,\dfrac{M.V_s}{L_s}\right)\dfrac{1}{L_r\sigma} \end{cases} \tag{32}$$

6.1 Control of the active powers

To control the power we set: $r=1$. The control of sliding surface of the active power can be written in the form:

$$\begin{cases} V_{rq}^{eq}=-\dfrac{L_s\,L_r\sigma}{M\,V_s}\dot{P}_s^{ref}+R_rI_{rq}+g\,\omega_sL_r\sigma I_{rd}+g\,\dfrac{M\,V_s}{L_s} \\ V_{rq}^{n}=L_r\,\sigma\,k_1\,sign\left(S\left(P\right)\right) \end{cases} \tag{33}$$

6.2 Control of the reactive power

The control of the sliding surface is defined by:

$$\begin{cases} V_{rd}^{eq}=L_r\sigma\left(\dfrac{V_s}{\omega_s\,M}-\dfrac{L_s}{V_s\,M}\dot{Q}_s^{ref}\right)+R_rI_{rd}-\mathrm{g}\omega_sL_r\sigma I_{rq} \\ V_{rd}^{n}=L_r\,\sigma k_2\,sign\left(S\left(Q\right)\right) \end{cases} \tag{34}$$

Where k_1 and k_2 are positives constants, $sign(S)$: Signum function. g : Slip. σ :Dispersion coefficient ($\sigma=1-M^2/L_sL_r$).

7. Fuzzy Sliding Mode Controller design

The conventional sliding mode controller produces high frequency oscillations in its outputs, causing a problem known as chattering. The chattering is undesirable because it can excite the high frequency dynamics of the system. To eliminate chattering, a continuous fuzzy logic control V^{fuz} is used to approximate the discontinuous control $k_i\ signs\ (S_i)$ (figure 9) [16].

Received: December 20, 2016

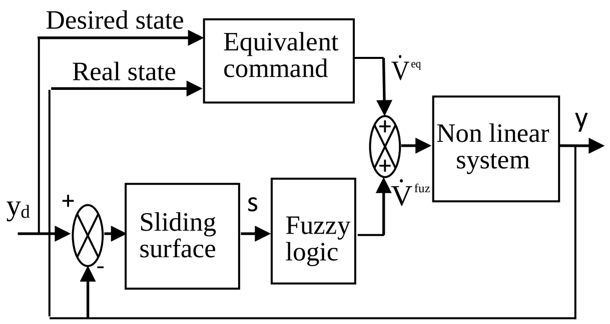

Figure.9 Fuzzy Sliding Mode control of the active and reactive power [16].

The fuzzy sliding mode controller (FSMC) is a modification of the sliding mode controller, where the switching controller term *sat(S(x))*, has been replaced by a fuzzy control input.

So voltage commands are obtained from equation system:

$$\begin{cases} \dot{V}_{rq} = \dot{V}_{rq}^{eq} + \dot{V}_{rq}^{fuz} \\ \dot{V}_{rd} = \dot{V}_{rd}^{eq} + \dot{V}_{rd}^{fuz} \end{cases} \tag{35}$$

To synthesis the fuzzy controller of two variables (active and reactive powers) fuzzy control uses a set of rules to represent how to control the system. The membership functions for input and output variables are given by figure 10 [17].

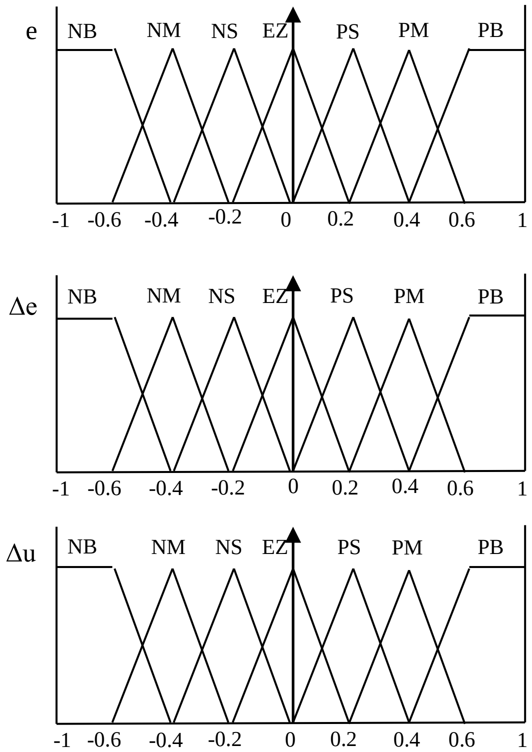

Figure.10 Membership for inputs and outputs.

NB : Negative Big, NS : Negative Small, NM : Negative Medium, PM : Positive Medium, PS : Positive Small, PB : Positive Big, EZ : Equal Zero.

The complete control rules used in our work are shown in table 1.

Table1. Rules table of the fuzzy controller [17].

e \ Δe	NB	NM	NS	EZ	PS	PM	PB
NB	NB	NB	NB	NB	NM	NS	EZ
NM	NB	NB	NB	NM	NS	EZ	PS
NS	NB	NB	NM	NS	EZ	PS	PM
EZ	NB	NM	NS	EZ	PS	PM	PB
PS	NM	NS	EZ	PS	PM	PB	PB
PM	NS	EZ	PS	PM	PB	PB	PB
PB	EZ	PS	PM	PB	PB	PB	PB

8. Results and discussion

To demonstrate the performance of the FSMC applied to a DFIG, we put it in the closest possible operating conditions to those of a wind system. The active power is controlled to follow the reference power; the latter is adapted to the wind speed by the MPPT, whereas the reactive power control allows us to get a unitary power factor. The parameters values of the wind turbine and the DFIG are shown in tables 2 and 3.

8.1 First Scenario: Sliding Mode Controller

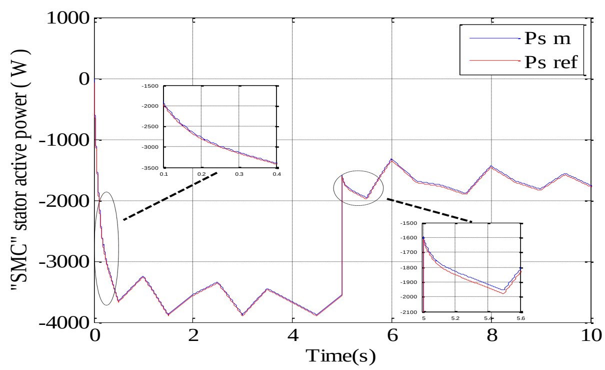

(a)

 DOI: 10.22266/ijies2017.0430.18

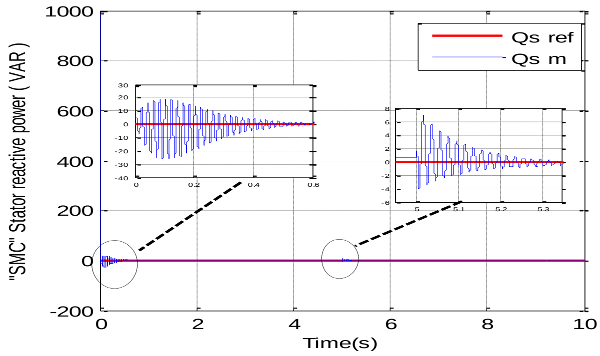

(b)

Figure.11 Active and reactive power of the DFIG for SMC Controller.

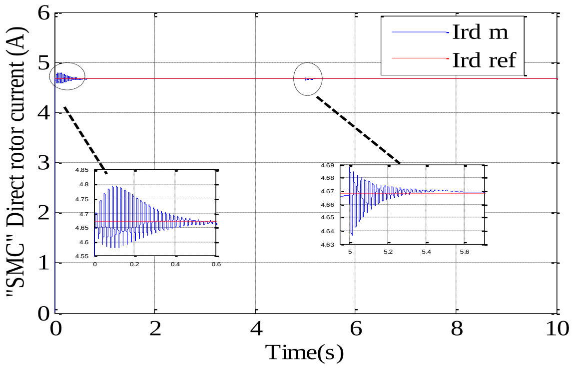

(a)

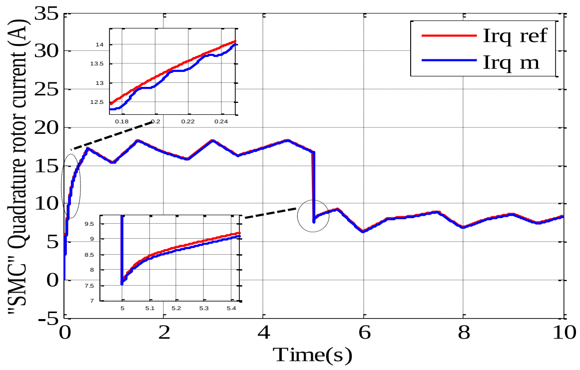

(b)

Figure.12 Direct and quadrature rotor currents of the DFIG for SMC Controller.

Figure 11 show the stator active and reactive powers and there references for SMC controller.

The reference of the stator active power is determined from the power of the turbine, we notes a follow-up of reference for the active power as well as the stator reactive power which is maintained null.

8.2 Second scenario: Fuzzy Sliding Mode Controller

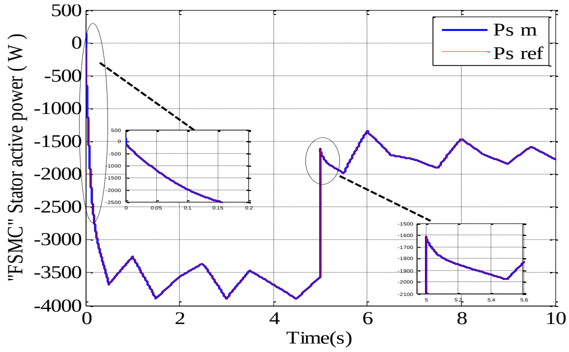

(a)

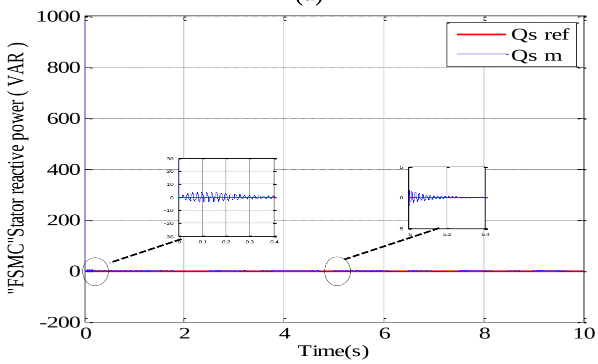

(b)

Figure.13 Active and reactive power of the DFIG for FSMC Controller.

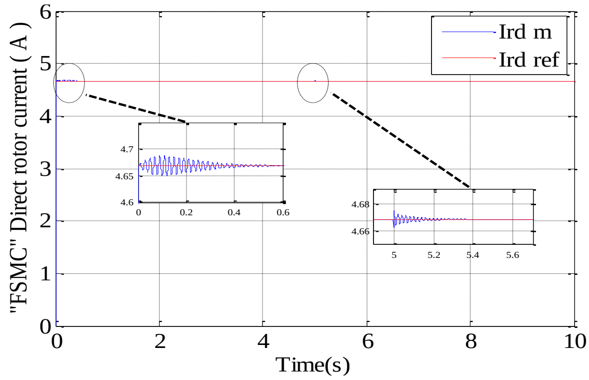

(a)

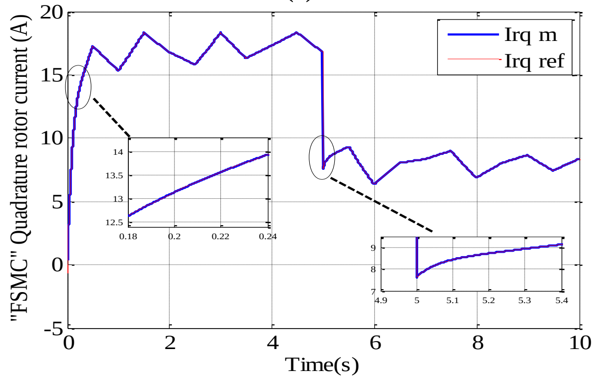

(b)

Figure.14 Direct and quadrature currents of the DFIG for FSMC controller.

These simulations (Figure 11 to 14) represent a comparison between the conventional sliding mode control and the fuzzy sliding mode control. To demonstrate the performance of the FSMC applied to a DFIG, we put it in the closest possible operating conditions to those of a wind system. The active power is controlled to follow the reference power. The latter is adapted to the wind speed by the MPPT, whereas the reactive power control allows us to get a unitary power factor. For the FSMC, the response time is significantly reduced and the oscillations are limited and damped more quickly compared to SMC controller. Simulations with this type of controller they showed very interesting performances in terms of reference tracking (time response, overshoot), sensitivity to perturbation.

9. Conclusion

This paper presents Hybrid Fuzzy Sliding Mode Control of active and reactive power in a DFIG and performance evaluations. After presenting a description of a doubly fed induction generator, a decoupling control method of active and reactive powers for DFIG has been developed. The description of the classical sliding mode controller (SMC) is presented in detail, this controller has been applied due to its excellent properties, such as insensitivity to certain external disturbances, however in standard sliding mode there is larger chattering. A hybrid fuzzy sliding mode approach using vector control strategy was established and presented. Responses of the system with the fuzzy sliding mode controller have shown that the last gives very interesting performances toward reference tracking, sensitivity to perturbation. The chattering free improved performance of the FSMC makes it superior to conventional SMC, and establishes its suitability for the system drive (are synthesized to perform powers reference tracking and efficient conversion).

Future work will focus on the use of other types of controllers, such as observer-based controllers, controllers based on higher-order sliding-mode neural networks and type-2 fuzzy logic in the domain of Direct Power Control (DPC) for DFIG-based wind power systems.

Appendix

Table 2. Wind turbine parameters.

Parameter	Definition	Value
R	Radius of the turbine	3 m
G	Gain multiplier	7.4
ρ	Air density	1.225 kg/m^3

Table 3. DFIG parameters.

Parameter	Definition	Value
P_n	Nominal power	4 KW
R_s	Stator resistance	1.2 Ω
R_r	Rotor resistance	1.8 Ω
L_s	Cyclic stator inductance	0.1554 H
L_r	Cyclic rotor inductance	0.1568 H
M	Mutual inductance	0.15 H
p	Number of pairs of poles	2
J	Inertia moment	0.2 kg.m^2
f	Friction coefficient	0.001 Nm.s

References

[1] L. Xiangjie, H. Yaozhen, “Sliding mode control for DFIG-based wind energy conversion optimization with switching gain adjustment”, *IEEE Proceeding of the 11th World Congress on Intelligent Control and Automation*, Shenyang, China, pp. 1213-1218, 2014.

[2] B. Hamane, M. L. Doumbia, M. Bouhamida, M. Benghanem, “Control of Wind Turbine Based on DFIG Using Fuzzy-PI and Sliding Mode Controllers”, *IEEE Proceedings Ninth International Conference on Ecological Vehicles and Renewable Energies (EVER),* Monte-Carlo (Monaco), French, pp. 440-448, 2014.

[3] E. Bogalecka, M. Kosmecki, “Control of reactive power in double-fed machine based wind park”, *IEEE 13th International Power Electronics and Motion Control Conference (EPE-PEMC*), Poznan, Poland pp. 1975-1980, 2008.

[4] T .Mesbahi, T. Ghennam, E.M. Berkouk, “A doubly fed induction generator for wind stand-alone power applications (simulation and experimental validation)”, *IEEE XXth International Conference on Electrical Machines (ICEM),* Marseille, France, pp.2028-2033, 2012.

[5] T. Ghennam, E.M. Berkouk, B. François, “Modeling and control of doubly fed induction generator (DFIG) based wind conversion system”, *IEEE, Second International Conference on Power Engineering, Energy and Electrical Drives (Powereng),* Lisbon, Portugal, pp. 507-512, 2009.

[6] S. EL-Aimani, B. Françoi, F. Minne, B. Robyns, “Modeling and simulation of doubly fed induction generators for variable speed wind turbines integrated in a distribution network”, *10th European conference on power electronics*

Received: December 20, 2016

and applications, (EPE), Toulouse, France, pp.1-10, 2003.

[7] T. Ghennam, E.M. Berkouk, “Back-to-back three-level converter controlled by a novel space-vector hysteresis current control for wind conversion systems”, *Electric Power System Research Journal, Elsevier,* Vol.80, Issue 4, pp. 444-455, 2010.

[8] M. Machmoum, F. Poitiers, C. Darengosse, A. Queric, “Dynamic performances of doubly-fed induction machine for a variable-speed wind energy generation”, *IEEE Proceedings of the International Conference on Power System Technology* , Vol.4, New York, NY, USA, pp. 2431-2436, 2002.

[9] R. Cheikh, H. Belmili, S. Drid, A. Menacer, M.Tiar, “Fuzzy logic control algorithm of grid connected doubly fed induction generator driven by vertical axis wind turbine in variable speed”, *IEEE Proceedings of the 3rd International Conference on Systems and Control, Algiers, Algeria,* pp. 439-444, 2013.

[10] E.S. Abdin, W. Xu, “Control design and dynamic performance analysis of a wind turbine induction generator unit”, *IEEE Transactions on energy conversion,* Vol.15, No.1, pp. 91-96, 2000.

[11] B. Boukhezzar, *“Sur les stratégies de commande pour l'optimisation et la régulation de puissance des éoliennes à vitesse variable ”*, Thèse de Doctorat, Université Paris XI UFR scientifique Orsay, France, 2006.

[12] V.I. Utkin, “Sliding mode control design principles and applications to electric drives”, *IEEE Transactions on Industrial electronics*, Vol. 40, Issue 1, pp.23-36, 2002.

[13] M. Bedboudi, H. Kherfane, D.E. Khodja, S. Moreau, “Sliding mode based fault tolerant control of an asynchronous machine”, *The Mediterranean Journal of Measurement and Control*, Vol.10, No.3, pp.284-291, 2014.

[14] S. Zeghlache, D. Saigaa, K. Kara, A. Harrag, A. Bouguerra “Fuzzy based sliding mode control strategy for an UAV type quadrator”, *The Mediterranean Journal of Measurement and Control,* Vol.8, No.3, pp. 436-446, 2012.

[15] A. Isidori, “*Nonlinear Control Systems*”, 3rd edition, Springer Verlag, London, 1995.

[16] A. Bouguerra , S. Zeghlache, K. Loukal, D. Saigaa “Fault tolerant fuzzy sliding mode controller of brushless DC motor (BLDC motor)” , *The Mediterranean Journal of Measurement and Control,* Vol.12, No.2, pp. 589-597, 2016.

[17] F. Boumaraf, “*Commande d’un aérogénérateur - Apport des techniques de l’intelligence artificielle*”, Thèse de Doctorat, Université de Batna, Algérie, 2014.